EVAPORATION EXPERIMENTS ON METALLIC IRON IN VACUUM

Akira TSUCHIYAMA and Seiji FUJIMOTO

Department of Earth and Space Science, Osaka University,
Toyonaka 560

Abstract: Evaporation experiments were carried out to examine evaporation kinetics of metallic iron, one of the important materials forming terrestrial planets and meteorites. Platelets of pure metallic iron were heated at temperatures ranging from 1075 to 1312°C under vacuum (10^{-5} to 10^{-6} Torr) for 0.5 to 96 hrs. The evaporation proceeds by forming evaporation steps, although small wüstite crystals were formed on the surfaces by partial oxidation of iron under vacuum. Amounts of evaporated iron estimated from mass loss of experimental charges increased with time at constant temperatures, showing a linear rate law. The evaporation rates, j, can be represented by $\ln j = 22.21 \pm 2.29 \,[\text{mol m}^{-2}\text{s}^{-1}] - 390.6 \pm 29.2 \,[\text{kJ mol}^{-1}] / RT$. The evaporation coefficients, α_v, were obtained by comparing the experimental results with calculated rates using the Hertz-Knudsen equation. The value of α_v is close to unity if effects of partial oxidation are taken into consideration. The present results give basic information for discussing chemical evolution of the primordial solar nebula.

1. Introduction

It is considered that evaporation and condensation of minerals which occurred in the primordial solar nebula were responsible for elemental and isotopic fractionations observed in the planets and meteorites. Especially, in recent nebula models (*e.g.*, NAKAGAWA and WATANABE, 1993), the evaporation process is important. In consequence of this, evaporation rates of minerals of cosmochemical importance have been measured in laboratories. In silicate systems, evaporation rates of forsterite have been measured in vacuum (HASHIMOTO, 1990; WANG *et al.*, 1993; TAKAHASHI *et al.*, 1993) and under H_2 atmospheres (NAGAHARA, 1994). Incongruent evaporation of enstatite was examined in the field of ceramics (SATA *et al.*, 1978). In metal-sulfide systems, TSUCHIYAMA *et al.* (1993) carried out incongruent evaporation experiments on FeS producing metallic iron residue, and discussed Fe/S fractionation in the primordial solar nebula together with the evaporation rates of metallic iron. However, they used the calculated rates for metallic iron because evaporation experiments of iron had not been done.

Evaporation rates are also important for discussing isotopic mass fractionation. DAVIS *et al.* (1990) showed large isotopic mass fractionation due to evaporation of forsterite melt into vacuum, and proposed that such fractionation is responsible for the observed isotopic fractionation in CAI's. It has been proposed that the isotopic mass fractionation due to evaporation is controlled by the balance between the evaporation rates and diffusion of isotopes in evaporated materials (DAVIS *et al.*,

1990; Wang *et al.*, 1993). Degrees of isotopic mass fractionations due to evaporation of minerals have been discussed based on the evaporation rates and diffusion coefficients in minerals (Nagahara, 1994; T. Takahashi *et al.*, in preparation).

In this study, evaporation experiments on metallic iron, one of the important materials forming terrestrial planets and meteorites, were carried out in vacuum to obtain the evaporation kinetics, such as mode and rates. The evaporation coefficients of metallic iron were evaluated from the results. The present data will give basic information on evaporation behavior of metallic iron in the primordial solar nebula, such as for discussing Fe/S fractionation by FeS evaporation and isotopic mass fractionation of Fe by evaporation.

2. Experiments

Plates of polycrystalline metallic iron of 99.99% purity were used in the present experiments. They were cut into platelets (about 0.5 mm thick and about 5×9 mm^2 in surface area), and the surfaces were polished. The starting materials were immersed in oil to avoid oxidation before runs. The samples were heated in a gold image furnace (ULVAC-RHV-E44VHT) at temperatures ranging from 1075 to 1312°C in vacuum for 0.5 to 96 hrs (Table 1). The temperature was controlled by a PID controller, and measured by a Pt-PtRd13 thermocouple. To eliminate reactions between the sample and the thermocouple, high-purity alumina was placed between

Table 1. Summary of the evaporation experiments of metallic iron.

Run #	Tempera-ture /°C	Duration /hr	Initial weight /mg	Final weight /mg	Weight loss, ΔM /mg	Surface area, S /mm^2	$\Delta M/S$ /mg mm^{-2}
1101	1075	72	150.45	149.51	0.94	94.260	0.010
1102	1075	96	159.72	154.87	4.85	98.895	0.0490
1103	1075	96	127.76	122.28	5.48	92.240	0.0594
1151	1123	72	103.60	93.50	10.10	85.255	0.1185
1153	1123	84	147.52	123.10	24.42	92.320	0.2645
1154	1123	84	161.18	138.72	22.46	99.410	0.2259
1152	1123	96	151.96	134.73	17.23	97.020	0.1776
1201	1170	24	138.82	128.20	10.62	91.020	0.1167
1202	1170	24	147.67	136.60	11.07	88.556	0.1250
1203	1170	24	140.52	128.49	12.03	95.050	0.1266
1204	1170	36	152.17	123.48	28.69	98.300	0.2919
1253	1220	4	154.02	137.94	16.08	91.540	0.1757
1251	1220	6	154.59	141.95	12.64	100.200	0.1262
1252	1220	8	137.59	117.30	20.29	93.525	0.2170
1303	1265	2	147.52	137.41	10.11	96.700	0.1046
1302	1265	4	142.50	124.64	17.86	92.830	0.1924
1301	1265	24	161.80	54.47	107.33	96.625	1.1108
1351	1312	0.5	132.11	125.29	6.82	90.280	0.0755
1353	1312	0.75	110.51	80.36	30.15	91.800	0.3284
1352	1312	1	133.68	110.47	23.21	89.485	0.2594

them. The vacuum was obtained by an oil diffusion pump, and the pressure ranged from 10^{-5} to 10^{-6} Torr.

The weight of the samples was measured before and after runs. The evaporation rates were obtained from the mass loss. The surfaces of the run products were observed under an SEM, and these chemical compositions were analyzed qualitatively with an EPMA (JEOL-733). The powder X-ray diffraction method was applied to the surfaces of the run products to determine the mineral phases exposed on the surfaces. As will be mentioned later, it was found that parts of the surfaces were oxidized and small wüstite crystals were formed on the surfaces. No corrections for this partial oxidation were made to the evaporation rates.

3. Results

Several features were observed on the surfaces of the run products. Networks of grooves were observed irrespective of the temperature (Fig. 1a, b, c). These grooves are considered to correspond to grain boundaries of polycrystalline iron formed by selective etching due to evaporation. The size of each single crystal ranges from a few tens to a few hundreds of μm. Holes, probably due to dislocations, were also observed (Fig. 1b). Steps were always observed on the surfaces (Fig. 1a, b, c). Each step runs through a single crystal domain. Facets of a single crystal have their own step directions and spacings (Fig. 1b, c). Martensite transformations from γ- to α-iron during cooling may cause stepped structures on the surfaces. However, it is hard to explain the observed features of the steps by martensite transformations because such steps should be formed along a specific crystallographic orientation irrespective of facet orientation. It is reasonable to consider that they are evaporation steps formed at screw dislocations and grain boundaries, and the evaporation proceeds by backward movement of these steps (HIRTH and POUND, 1963). The original surfaces of the starting materials etched by a dilute solution of HCl have a texture composed of fine laths of sub-μm in size. Such texture should be formed by the martensite transformation.

Euhedral crystals of about 10 μm size are always attached to the stepped surfaces. Occasionally, the crystals show beautiful pyramidal shapes, which are halves of octahedrons (Fig. 1d). Powder X-ray diffraction patterns and qualitative chemical analyses showed that they are wüstite. The wüstite crystals cover ten to a few tens % of the entire surfaces on average, and more than a few tens of % in some regions (Fig. 1e). It is also observed that the wüstite crystals sometimes interact with the evaporation steps (Fig. 1f). Under the vacuum conditions in the experiments (about 10^{-5} to 10^{-6} Torr), the partial pressure of oxygen, p_{O_2}, should be about 10^{-9} atm (3×10^{-9} to 3×10^{-10} atm) if residual gas is assumed to be composed of air. Back diffusion of oil used in the diffusion pump may affect p_{O_2}. Because the oil acts as a reducing agent, p_{O_2} should be slightly less than 10^{-9} atm. In such a range of the oxygen partial pressure, wüstite and magnetite are stable at high and low temperatures in the experiments, respectively (Fig. 2). Accordingly, wüstite was formed by oxidation of metallic iron even under vacuum. Magnetite was not detected probably because the oxidation reaction did not go to completion.
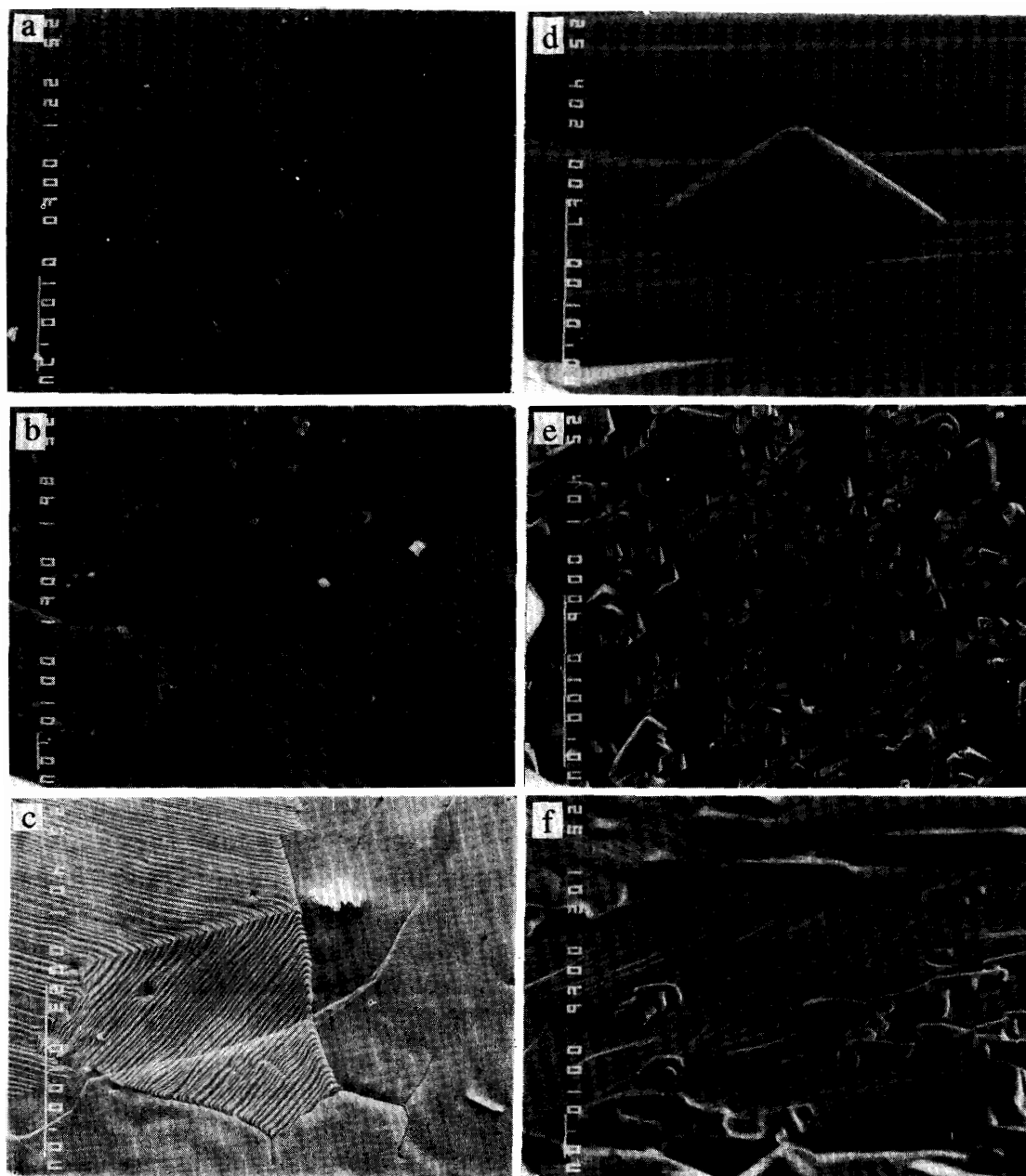
Fig. 1. SEM micrographs of the surfaces of run products.

(a) Grain boundaries and evaporation steps at 1123°C for 96 hrs (run#1152). The scale bar is 100 μm.

(b) Close up of (a). Coarse or fine (sometimes very fine) steps are observed in each single crystal region. Holes probably formed along dislocations are also seen. Some steps are so fine that it is hard to recognize these steps in this micrograph, but they can be observed under higher magnifications. The scale bar is 10 μm.

(c) Grain boundaries and evaporation steps at 1170°C for 24 hrs (run#1201). The scale bar is 100 μm.

(d) A wütite crystal with a pyramidal shape attached on a stepped surface at 1075°C for 96 hrs (run#1103). The micrograph was taken from an oblique angle. The scale bar is 10 μm.

(e) A surface covered with a large amount of wütite crystals at 1170°C for 24 hrs (run#1203). The scale bar is 100 μm.

(f) Interaction between evaporation steps and wütite crystals at 1075°C for 96 hrs (run#1103). The micrograph was taken from an oblique angle. The scale bar is 10 μm.
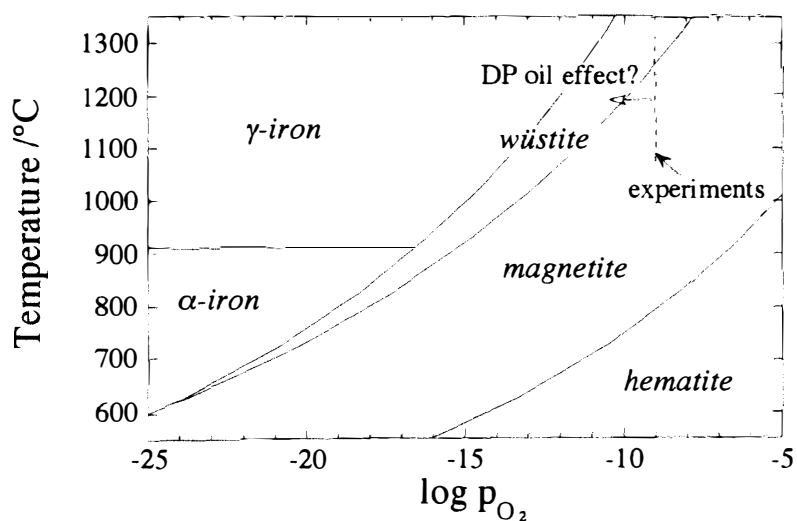
Fig. 2. *Temperature-oxygen partial pressure, p_{O_2}, conditions of the present experiments shown in the phase diagram of the system Fe-O. The phase diagram was made from thermochemical data of JANAF (1971), and is essentially the same as published phase diagrams. Metallic iron can be oxidized to form wüstite or magnetite under the experimental conditions. p_{O_2} in the experiments is assumed from residual oxygen gas during evaporation. A possible effect of reduction by back diffusion of diffusion pump (DP) oil is also taken into consideration.*
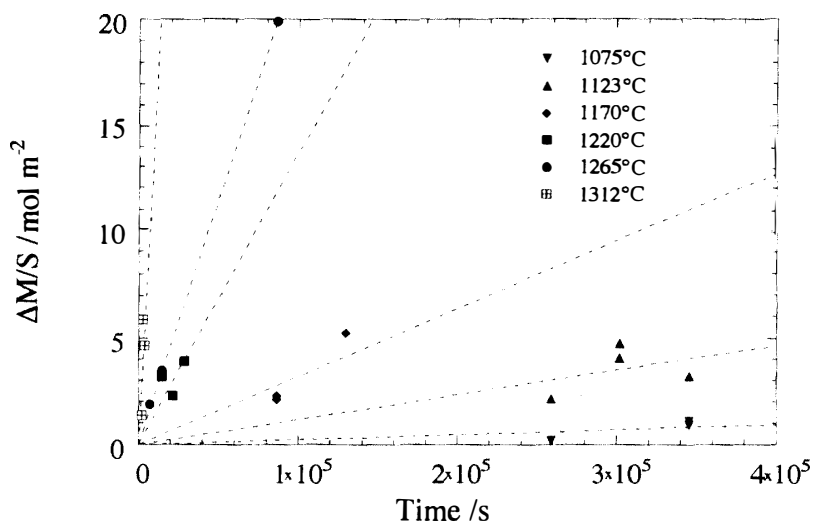

Fig. 3. *Mass loss of experimental charges per unit area, $\Delta M/S$, as a function of time by evaporation of metallic iron into vacuum at different constant temperatures.*

Mass loss of an experimental charge per unit area, $\Delta M/S$, is plotted against time, t (Fig. 3; also see Table 1). The mass loss is roughly proportional to time at constant temperature although there is some scatter. This shows that iron evaporation

Table 2.   Measured evaporation rates, j_{meas}, of metallic
            iron in vacuum and their standard deviations
            obtained from the present experiments.

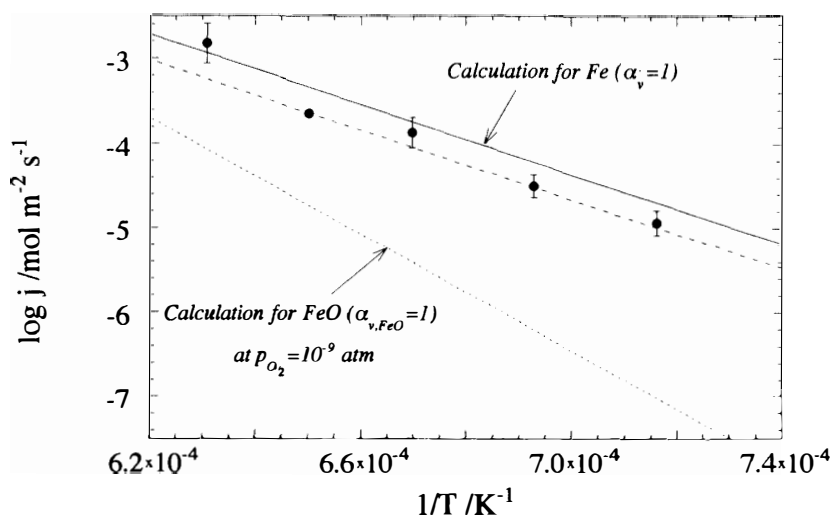| Temperature /°C	j_{meas} /mol m^{-2} s^{-1}	Standard deviation /mol m^{-2} s^{-1}
1075	2.344×10^{-6}	6.43×10^{-7}
1123	1.165×10^{-5}	1.72×10^{-6}
1170	3.182×10^{-5}	4.27×10^{-6}
1220	1.370×10^{-4}	2.49×10^{-5}
1265	2.307×10^{-4}	1.99×10^{-6}
1312	1.491×10^{-3}	3.49×10^{-4}

Fig. 4.   Arrhenius relation of the evaporation rates of metallic iron obtained
           from the slopes of the $\Delta M/S$-t relation in the experiments. A thick
           dashed line shows a linear regression of the weighted data on the
           evaporation rates obtained in the present experiments (Table 2). The
           calculated rate, j_{calc}, with $\alpha_v = 1$ according to eq. (3) (solid line), and
           that for FeO at p_{O_2} of 10^{-9} atm with $\alpha_{v,FeO} = 1$ according to eq. (5)
           (thin dashed line) are also shown.

obeys a linear rate law. The evaporation rates (mol of Fe per unit area and unit time),
j_{meas}, were obtained from the $\Delta M / S$-t slopes by a least square method by assuming
$\Delta M / S = M_{Fe}\, j_{meas}\, t$, where M_{Fe} is the molar weight of iron. The values of j_{meas} are
listed in Table 2 together with their standard deviations. The presence of wüstite due
to partial oxidation on the surface affects the evaporation rates as discussed later.
Quantitative corrections to the evaporation rates for the partial oxidation effects were
not made here.

The evaporation rates increase with increasing temperature. An Arrhenius plot
of the evaporation rates is shown in Fig. 4. A linear regression of the weighted data
(Table 2) shows that the evaporation rates can be represented by

$$\ln j_{\text{meas}} = 22.21 \pm 2.29 \, [\text{mol m}^{-2}\text{s}^{-1}] - 390.6 \pm 29.2 \, [\text{kJ mol}^{-1}] / RT, \quad (1)$$

where R is the gas constant, and T is temperature.

4. Discussion

Body-centered cubic (b.c.c.) α-iron transforms to γ-iron (f.c.c.) at 911°C, and γ-iron to δ-iron (b.c.c.) at 1392°C: δ-iron melts at 1536°C. In the temperature range of the experiments (1075–1312°C), γ-iron is stable. Accordingly, it is reasonably considered that the evaporation behavior of γ-iron was observed in the present experiments.

The evaporation reaction of metallic iron can be expressed as follows:

$$\text{Fe}(s) = \text{Fe}(g), \quad (2)$$

where s and g denote solid and gas, respectively. In this reaction, it is assumed that monomolecules of iron, Fe(g), are formed by the evaporation. Because this reaction does not contain H_2, the evaporation of metallic iron should not be affected by the partial pressure of H_2, p_{H_2}. Therefore, the evaporation rates of metallic iron into vacuum obtained in the present experiments can be applicable to those under an H_2-rich atmosphere, such as in the primordial solar nebula.

The evaporation rates of metallic iron, j_{calc}, can be calculated from the Hertz-Knudsen equation (e.g., HIRTH and POUND, 1963):

$$j_{\text{calc}} = \frac{\alpha_v \, p_{\text{Fe}}}{N_A \, \sqrt{2\pi m_{\text{Fe}} kT}}, \quad (3)$$

where α_v is the evaporation coefficient, p_{Fe} the equilibrium pressure of Fe(g), m_{Fe} the mass of the molecule, N_A the Avogadro number, and k the Boltzmann constant. The value of the evaporation coefficient, α_v, is between zero and unity, depending on the evaporation kinetics. If any kinetic constraint is absent, it becomes unity as the maximum value (HIRTH and POUND, 1963). SATA et al. (1978) measured evaporation coefficients of simple solid oxides, such as Al_2O_3, and showed that α_v decreases from unity to 10^{-2} with decreasing temperature from the melting points, T_m. If the data for Al_2O_3 is extrapolated to the temperature of $T_m / 1.5$, α_v becomes 10^{-4}. On the other hand, it is generally considered that α_v might be close to unity for metals because the kinetic constraints for metals are expected to be small.

The values of p_{Fe} can be calculated from the reaction constant of eq. (2), K_{Fe}:

$$p_{\text{Fe}} = K_{\text{Fe}} = \exp\left(-\Delta G^\circ / kT\right), \quad (4)$$

where ΔG° is the standard free energy of reaction, and was obtained from thermochemical data (JANAF, 1971) as a function of temperature. The evaporation rates with $\alpha_v = 1$ were calculated from eqs. (3) and (4), and are shown in Fig. 4 as a solid line. The evaporation rates obtained in the present experiments, j_{meas}, are

slightly smaller than the calculated rates. If we assume that $j_{meas} = \alpha_v j_{calc}$, α_v becomes about 0.5 (ln $\alpha_v = -0.890 + 299 / T$). Strictly speaking, the temperature dependence of the measured and theoretical evaporation rates, j_{meas} and j_{calc}, in eqs. (1) and (3), respectively, are slightly different. The Arrhenius relation is assumed in eq. (1), while the $1 / \sqrt{T}$ term is added to the exponential temperature dependence of the Arrhenius expression in eq. (3). However, this $1 / \sqrt{T}$ dependence is much smaller than the exponential temperature dependence. Therefore, we neglected the $1 / \sqrt{T}$ dependence, and obtained α_v by comparing j_{meas} directly with j_{calc}.

The presence of wüstite due to partial oxidation on the surfaces affects the measured evaporation rates. The evaporation rates of FeO, j_{FeO}, can also be calculated from the Hertz-Knudsen equation:

$$j_{FeO} = \frac{\alpha_{v,FeO} K_{FeO}}{N_A \sqrt{2\pi m_{Fe} kT p_{O_2}}},$$ (5)

where $\alpha_{v,FeO}$ is the evaporation coefficient, and K_{FeO} is the reaction constant of the evaporation reaction:

$$FeO(s) = Fe(g) + \frac{1}{2} O_2(g).$$ (6)
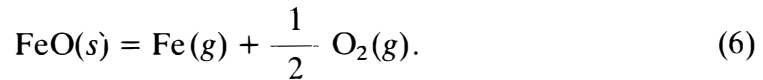
From eqs. (3), (4) and (5), the ratio of the theoretical evaporation rates for FeO and Fe, j_{FeO} / j_{calc} can be obtained as follows:

$$\frac{j_{FeO}}{j_{calc}} = \left(\frac{\alpha_{v,FeO}}{\alpha_v}\right) \left(\frac{a_{Fe}}{a_{FeO}}\right),$$ (7)

where a_{Fe} and a_{FeO} are the activities of Fe and FeO, respectively. This shows that wüstite is more refractory than metallic iron if wüstite is more stable than iron. The evaporation rate at p_{O_2} of 10^{-9} atm was calculated with thermochemical data (JANAF, 1971), and is lower than that of metallic iron by one order of magnitude or more (Fig. 4). Accordingly, wüstite can be formed on the surfaces without evaporation by partial oxidation. The presence of wüstite reduces effective surface area for the evaporation of metallic iron. Therefore, the real evaporation rates of the metallic iron should be larger than the uncorrected evaporation rates, and thus the real evaporation coefficients, α_v, should be larger than those obtained from the uncorrected rates. The mass loss is also affected by the formation of wüstite. The real evaporation rates and thus α_v are also larger than the uncorrected values due to extra oxygen in wüstite. It is difficult to correct the evaporation rates precisely. However, when a few tens of % of the surface area are covered with wüstite crystals of about 10 μm, the evaporation coefficients of metallic iron, α_v, in the present experiments should be close to unity. It is generally expected that values of α_v are close to unity as already mentioned. The present results confirm this general expectation.

Tsuchiyama et al. (1993) measured evaporation rates of FeS under H_2 atmosphere, and found that the incongruent evaporation of FeS obeys a linear rate law due to formation of porous metallic iron as the evaporation residue. They compared the rates of metallic iron formation by the FeS incongruent evaporation with calculated evaporation rates of metallic iron with $\alpha_v = 1$, and discussed Fe / S

fractionation by FeS evaporation. It is expected that the incongruent evaporation rates of FeS decrease with decreasing p_{H_2}, while the evaporation rates of iron are not affected by p_{H_2}. Therefore, FeS could evaporate congruently without formation of iron residue at high temperatures near the Fe-FeS eutectic and low H_2 pressures, where the evaporation rates of iron exceed the rates of metallic iron formation. In this case, Fe / S fractionation by FeS evaporation is not expected. If α_v for metallic iron is smaller than unity, such congruent evaporation of FeS due to the kinetic effect is difficult. The present results suggest that the kinetic congruent evaporation of FeS might occur if specific regions with low p_{H_2} and high temperatures were present in the solar nebula. Isotopic mass fractionation of Fe due to evaporation of γ-iron can also be discussed based on the present results with the diffusion coefficient of Fe in γ-iron (T. TAKAHASHI, in preparation).

Acknowledgments

References

DAVIS, A. M., HASHIMOTO, A., CLAYTON, R. N. and MAYEDA, T. K. (1990): Isotope mass fractionation during evaporation of Mg_2SiO_4. Nature, **347**, 655–658.

HASHIMOTO, A. (1990): Evaporation kinetics of forsterite and implications for the early solar nebula. Nature, **347**, 53–55.

HIRTH, J. P. and POUND, G. M. (1963): Condensation and Evaporation, Nucleation and Growth Kinetics. Pergamon, 191p.

JANAF Thermochemical Tables, 2nd ed. (1971): National Bureau of Standards, U.S.A., NSRDS-NBS37, 1141p.

NAKAGAWA, Y. and WATANABE, S. (1993): Origin of the solar system. Sciences for Planets, ed. by M. SHIMIZU. Tokyo, Asakura, 185–219 (in Japanese).

NAGAHARA, H. (1994): Kinetics of evaporation and fractionation with hydrogen of forsterite. Papers Presented to the 19th Symposium on Antarctic Meteorites, May 30–June 1, 1994. Tokyo, Natl Inst Polar Res., 75–77.

SATA, T., SASAMOTO, T., LEE, H. L. and MAEDA, E. (1978): Vaporization processes from magnesium materials. Rev. Int. Hautes Temp. Refract., Fr., **15**, 237–248.

TAKAHASHI, T., TSUCHIYAMA A. and UYEDA, C. (1993): A measurement of evaporation rates of forsterite (Mg_2SiO_4). 1993 Fall Meeting of The Japanese Society of Planetary Sciences (abstract), 161 (in Japanese).

TSUCHIYAMA, A., UYEDA, C. and MAKOSHI, Y. (1993): An experimental study of evaporation of FeS, and cosmochemical significance. Papers Presented to the 18th Symposium on Antarctic Meteorites, May 31–June 2, 1993. Tokyo, Natl Inst Polar Res., 121–124.

WANG, J., DAVIS, A. M., HASHIMOTO, A. and CLAYTON, R. N. (1993): Diffusion-controlled magnesium isotopic fractionation of a single crystal forsterite evaporated from the solid state. Lunar and Planetary Science XXIV. Houston, Lunar Planet. Inst., 1479–1480.